Title
A STUDY OF THE REACTIONS K~ + p-^K + N (y)

Author
Graziano, William.

Publication Date
1962-03-19

UCRL 10126

University of California

Ernest O. Lawrence Radiation Laboratory

A STUDY OF THE REACTIONS $K^- + p \rightarrow K + N + (\pi)$ AT 1.15 Bev/c

Berkeley, California

DISCLAIMER

Research and Development

UCRL-10126
UC-34 Physics
TID-4500 (17th Ed.)

UNIVERSITY OF CALIFORNIA
Lawrence Radiation Laboratory
Berkeley, California

Contract No. W-7405-eng-48

A STUDY OF THE REACTIONS $K^- + p \rightarrow \bar{K} + N + (\pi)$ AT 1.15 Bev/c

William Graziano

(Ph. D. Thesis)

March 19, 1962

A STUDY OF THE REACTIONS $K^- + p \rightarrow K + N + (\pi)$ AT 1.15 Bev/c

Contents

A STUDY OF THE REACTIONS $K^- + p \rightarrow \overline{K} + N + (\pi)$ at 1.15 Bev/c

William Graziano

(Ph. D. Thesis)

Lawrence Radiation Laboratory
University of California
Berkeley, California

March 19, 1962

ABSTRACT

This report describes a study of the following $K^- p$ reactions at 1.15 Bev/c:

$$\begin{aligned} K^- + p &\rightarrow K^- + p \\ &\rightarrow \overline{K^0} + n \\ &\rightarrow K^- + p + \pi^0 \\ &\rightarrow K^- + n + \pi^+ \\ &\rightarrow \overline{K^0} + n + \pi^0 . \end{aligned}$$

Cross sections for each of these reactions and angular distributions for the elastic and charge-exchange scatters are presented. From the analysis of the $K^- p \pi^0$ events, we obtained the cross section for the reaction $K^- + p \rightarrow K^{*-} + p$, with the K^{*-} decaying into $K^- + \pi^0$. Combining this cross section with that for $K^- + p \rightarrow K^{*-} + p$ followed by $K^{*-} \rightarrow \overline{K^0} + \pi^-$, we find a value of 0.5±0.2 for the branching ratio, $(K^{*-} \rightarrow K^- + \pi^0)/(K^{*-} \rightarrow \overline{K^0} + \pi^-)$. This value substantiates the earlier preliminary result of isotopic spin 1/2 for the K^* resonance.

I. INTRODUCTION

During the Fall of 1958, the Lawrence Radiation Laboratory's 15-in. hydrogen bubble chamber was exposed to a separated beam of 1.15-Bev/c K^- mesons. A systematic study was undertaken of the interactions produced by the approximately 100,000 K^- mesons that entered the bubble chamber. Partial results of this study are contained in references 1 through 4. In this paper, we present data for the following reactions:

$$
\begin{aligned}
K^- + p &\rightarrow K^- + p \\
&\rightarrow \overline{K^0} + n \\
&\rightarrow K^- + p + \pi^0 \\
&\rightarrow K^- + \pi^+ + n \\
&\rightarrow \overline{K^0} + n + \pi^0 .
\end{aligned}
$$

These reactions can appear as either V^0 zero-prong or as two-prong events (see Figs. 1 and 2). Unfortunately, a relatively large number of other reactions can produce these two configurations. Section IV describes the separation of these $\overline{K}N$ and $\overline{K}N\pi$ events from the events produced by other reactions and the corrections required to remove certain biases from the data.

The cross sections for the above five reactions and angular distributions for the first two reactions are presented in Section V. Also, information obtained from our $\overline{K}N\pi$ events on the spin and isotopic spin of the K^* resonance is presented in that section.[3]

Section III contains a brief description of the K^- beam and a discussion of the scanning, measuring, and kinematical analysis of our bubble-chamber events.

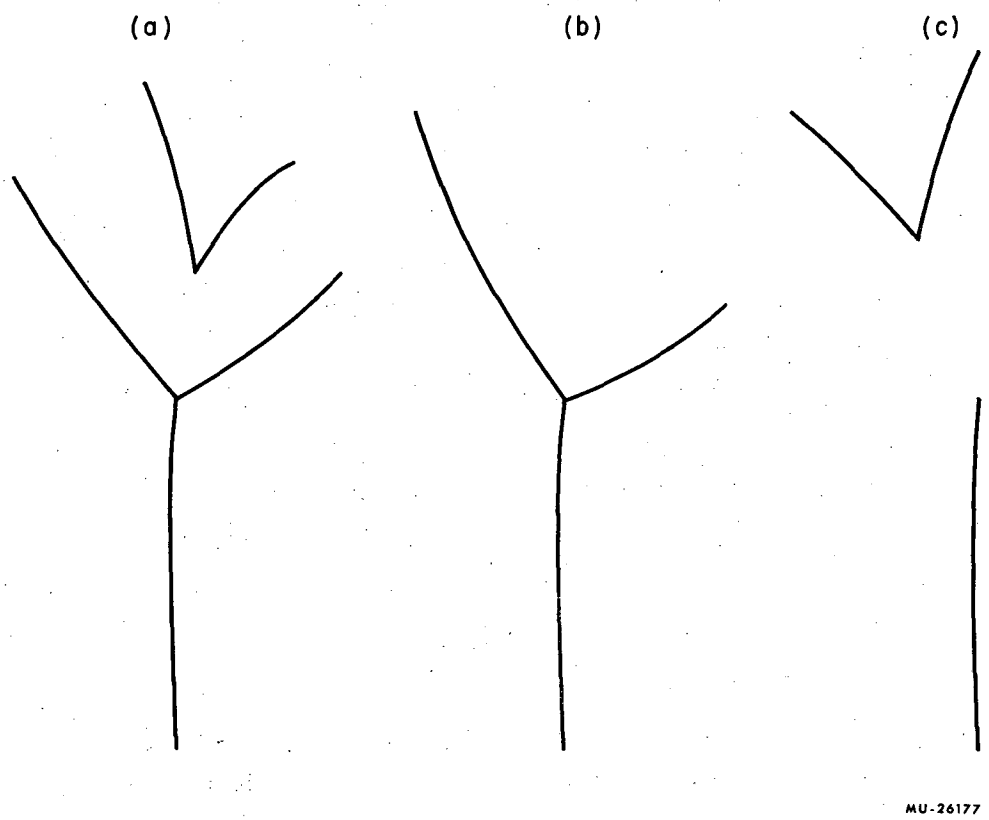

Fig. 1. Illustrations of (a) V^0 two-prong, (b) two-prong, and (c) V^0 zero-prong event types.

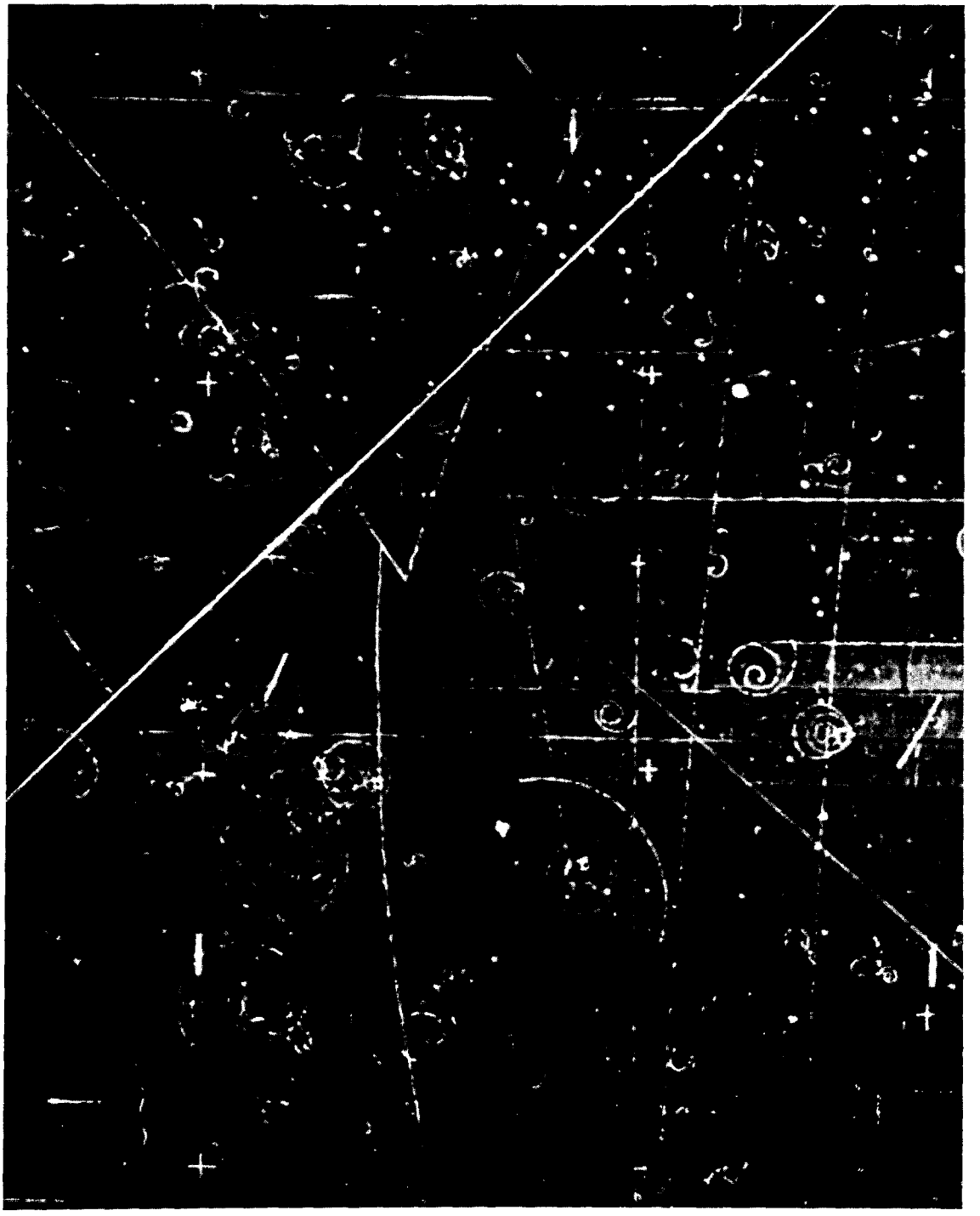

ZN-3090

Fig. 2 Bubble-chamber picture showing a two-prong event.

II. EXPERIMENTAL PROCEDURE

A. The K^- Beam

The K^- beam used in this experiment has been described in detail elsewhere;[5,6] thus we will only summarize some of its more important characteristics. A schematic drawing of the beam is shown in Fig. 3. The beam was designed to accept negatively charged particles from the Bevatron in the momentum interval from 1155 to 1185 Mev/c; in traveling from the Bevatron to the bubble chamber, the momentum of these particles was reduced by approximately 20 Mev/c. Two stages of electrostatic separation were used to separate the K^- mesons from the other particles in the beam.

A preliminary analysis of the ratio of π^- to K^- mesons was made by searching for incident tracks that interacted in the bubble chamber and which had a δ ray with energy greater than 5.83 Mev. These tracks must be π^- mesons, since the maximum δ-ray energy that a 1.15-Bev/c K^- meson can produce is 5.83 Mev. The results were that the ratio of π^- to K^- was either 50 ± 18% or 8 ± 11% depending on how we chose to operate the beam.[5] The purpose of the 50% π^--to-K^- operating condition was to increase the K^--meson flux.

To determine the collimation of the beam K^- mesons, we analyzed our τ decay events. In approximately 93% of these events, the direction of the incident K^- meson was within ± 2.4 deg in azimuth and ±2.4 deg in dip of a certain fixed direction in space (approximately the average direction of our τ mesons). Therefore, by requiring that the incident track of an interaction be within ±2.4 deg in azimuth and dip of this direction, we were able to reduce the number of events produced by π^- mesons and K^- mesons that had scattered in the beam. In the analysis of our K-p elastic scatters (discussed later in this paper), the smaller of the π^--to-K^- ratios was calculated for the particles that satisfied this beam criterion.

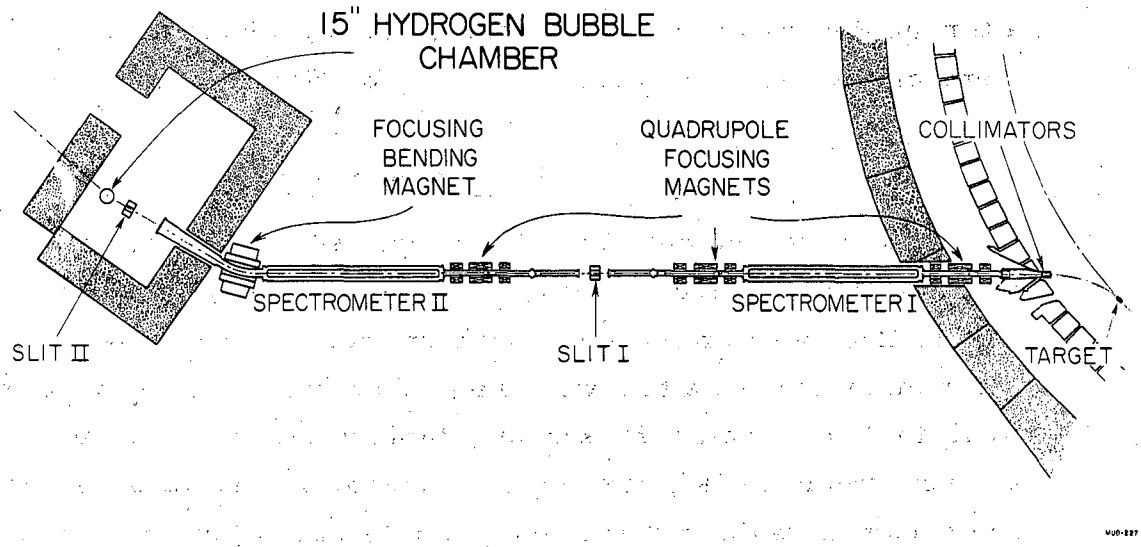

Fig. 3. Schematic drawing of the K^- beam used in this experiment.

The average momentum and momentum spread of the K^- mesons was determined by studying our $K\mu_2$ decays in which the muon stopped. Since the direction of a particle can be measured very accurately in a bubble chamber, and because for these events the momentum of the muon can be precisely determined from its range, we can calculate the momentum of the incident K^- meson with an error of only about 5 Mev/c. We had 46 decays in which a muon stopped; three of these did not satisfy our angle criterion for beam tracks. The average momentum for the remaining 43 decays was 1150 ± 3 Mev/c and the spread was ±20 Mev/c, after unfolding experimental errors. This analysis of our beam momentum has been discussed thoroughly by Wojcicki.[6]

B. Processing of Data

Each bubble chamber picture was scanned twice for incident tracks that interacted or decayed. The purpose of the second scan was both to find events missed on the first scan and to enable us to estimate the number of events that were missed on both scans. Since it is difficult to determine on the scanning table whether the incident track of an event would satisfy our angle criterion, we retained all interactions and decays in which the incident particle was within approximately ±5.0 deg in azimuth and dip of the beam direction. The remaining non-beam events were eliminated after the events were measured. Also, the events were examined by the scanner to determine whether they were within a specified fiducial volume defined by using the optical markers on the top glass as reference points. Events outside of this volume are usually difficult to analyze and were therefore rejected.

Unfortunately, at this momentum it is impossible to determine by visual inspection the reaction that produced an event; the event must be fitted to the possible interpretations before the correct one can be determined. Thus, during the scanning no effort was made to identify the reaction that produced an event. Instead, each event was placed according to its topology into one of eight classifications, called event types. Some of these event types are illustrated in Fig. 1.

From the four available bubble-chamber pictures of an interaction, we selected for each track of an event the two views that would give the most accurate spatial reconstruction of the track. A projection microscope, called Franckenstein,[7] was used to obtain the film coordinates of several points on each track in the two views selected.

PANG, a program for the I. B. M. 704, utilized these film coordinates to reconstruct each of the tracks in space.[8] Using the event type of the interaction, PANG assigned masses to the particles that produced the tracks. The momentum and space angles, along with their errors, were then calculated for each particle.

A program, KICK,[9] used the data provided by PANG on a given event to perform a least-squares fit to each of the possible interpretations for this event. It used the four energy-momentum conservation equations as the constraints. For each hypothesis, KICK calculated the χ^2, the fitted momenta and angles for the particles, and the errors on the fitted data. If the incident particle in a given hypothesis was a K^- meson, then before it performed the fit KICK would average the momentum obtained from PANG with 1150 ± 20 Mev/c. This was done, because the error on the measured momentum of a 1 Bev/c particle is frequently quite large. A given interpretation was rejected if its χ^2 value corresponded to a probability of less than 1%.

A program named EXAMIN was written to perform special calculations on the fitted data from KICK. Since the calculations performed by EXAMIN depend upon the event type, we will discuss them in the section on the analysis of the data.

C. The K^- Pathlength

The total K^- pathlength for this experiment was calculated from the number of K^- decays which had a decay angle in the laboratory system greater than 4 deg. The method used for this analysis is discussed elsewhere.[6] The cross section for one event in our entire film sample was found to be 12.2 μb. In the restricted film sample for which the π^--to-K^- ratio was 8±11%, one event corresponded to 30.3μb. Errors associated with the above two numbers are not given because they are insignificant compared to the errors associated with the number of interactions.

III. ANALYSIS OF EVENTS

A. $\overline{K^0}n$ and $\overline{K^0}n\pi^0$ Events

The following reactions can produce a V^0 zero-prong configuration in a hydrogen bubble chamber:

$$K^- + p \rightarrow \overline{K^0} + n \quad (1)$$
$$\rightarrow \overline{K^0} + n + \pi^0 \quad (2)$$
$$\rightarrow K^0 + n + 2\pi^0 \quad (3)$$
$$\rightarrow \Lambda + a\,\pi^0 \quad a \geq 1 \quad (4)$$
$$\rightarrow \Sigma^0 + a\,\pi^0 \quad a \geq 1 \quad (5)$$
$$\pi^- + p \rightarrow \overline{K^0} + \Lambda \quad (6)$$

Since V^0 zero-prong events with a very short V^0 can be mistaken for two-prong events and are difficult to analyze, we adopted a cutoff length of 0.4 cm and rejected all events in which the V^0 traveled less than this distance in the chamber. In addition, the events in which the V^0 decayed outside of our fiducial volume were eliminated, since it is very difficult to analyze the decay of the V^0 for these events. In calculating the cross sections and angular distributions, corrections were made for the V^0 events in which the V^0 decayed outside of our fiducial volume or within 0.4 cm of the point of production.

To separate the $\overline{K^0}$ events from the Λ events, we fitted the V^0 to both the $\overline{K^0}$ and the Λ decay hypotheses. In addition, we examined the ionization of the positive track and checked to see if the fitted data on the $\overline{K^0}$ and Λ interpretations were within the kinematical limits for the production processes. This procedure always enabled us to distinguish between the two decay hypotheses for an event.

In our entire film sample we have approximately 350 V^0 zero-prong events; in 133 of these the V^0 was found to be a $\overline{K^0}$ decay. We fitted each of these $\overline{K^0}$ events to a $K^- + p \rightarrow \overline{K^0} + n$ interpretation, using the direction and momentum for the $\overline{K^0}$ obtained from the decay fit. Reactions (2) and (3) cannot be fitted, since they have more than one missing neutral track. However, we did calculate for each event the mass, M_m, of the missing neutral-particle system

$$M_m^2 = (E_{\overline{K^0}} - E_{K^-} - M_p)^2 - (P_{\overline{K^0}} - P_{K^-})^2 .$$

A typical error for M_m would be about 20 Mev. If an event were due to reaction (2) or (3), then M_m would have to be greater than or equal to the mass of a neutron, M_n, plus the mass of a π^0 meson, M_π. One hundred seven of the $\overline{K^0}$ events fitted reaction (1), and for each of these events M_m was less than $M_n + M_\pi$, indicating that they could not be due to reactions (2) and (3). Twenty-six events did not fit hypothesis (1), and M_m for all of these events was greater than $M_n + M_\pi$. Thus we were able to separate the events produced by reaction (1) from those due to reactions (2) and (3). A histogram of M_m for the 133 $\overline{K^0}$ events is shown in Fig. 4.

We probably do not have any $\overline{K^0}$ zero-prong events produced by reaction (3), since in our $\overline{K^0}$ two-prong events we have no examples of the reactions $K^- + p \rightarrow \overline{K^0} + n + \pi^+ + \pi^-$ and $K^- + p \rightarrow \overline{K^0} + p + \pi^+ + \pi^-$. Also, since we have only two events due to reaction (6) in which two V^0 decays are visible, we probably have no more than one or two examples of reaction (6) among our $\overline{K^0}$ zero-prong events. Thus almost all of our $\overline{K^0}$ zero-prong events are due to reactions (1) and (2), 107 being produced by reaction (1) and 26 by reaction (2).

To obtain the total number of K^0N and $\overline{K^0}N\pi^0$ events produced, we used our EXAMIN program to calculate for each event the probability p that the $\overline{K^0}$ would decay by the charged mode within our fiducial volume and have traveled more than 0.4 cm. Each event was then weighed by 1/p. We did not have to make any correction for events missed on the two scans, because the scanning efficiency for the V^0 events that we accepted is very nearly 100%.

Summing the weights for the events, we found that we had 432 $\overline{K^0}N$ and 106 $\overline{K^0}N\pi^0$ events. A histogram for the angular distribution of the $\overline{K^0}N$ events (including the 1/p correction factors) is given in Fig. 5.

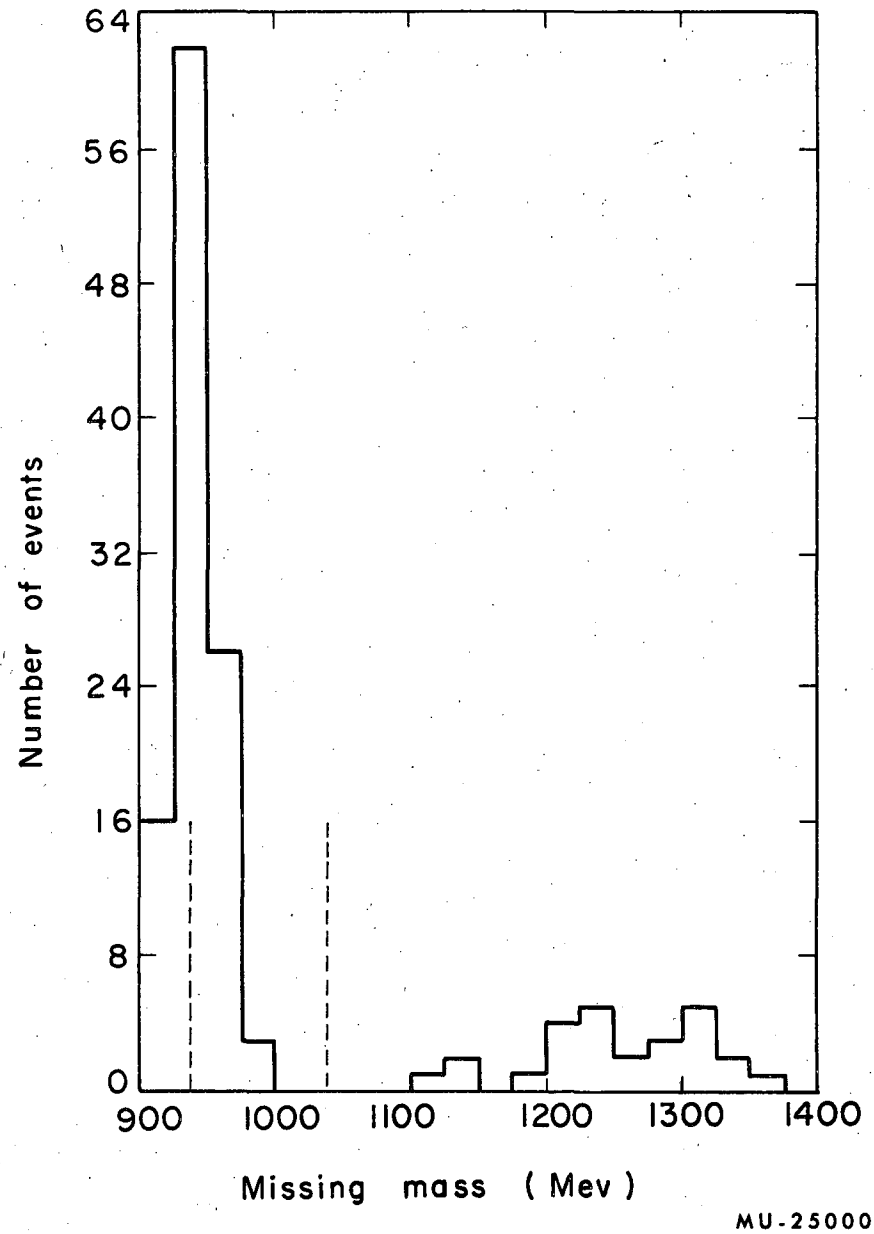

Fig. 4. Mass of the missing-neutral system for the $\overline{K^0}$ zero-prong events. The dotted line on the left (at 940 Mev) represents the expected value of the missing mass for the $\overline{K^0}N$ events. The dotted line on the right (at 1080 Mev) represents the lower limit of the missing mass for $KN\pi$ events.

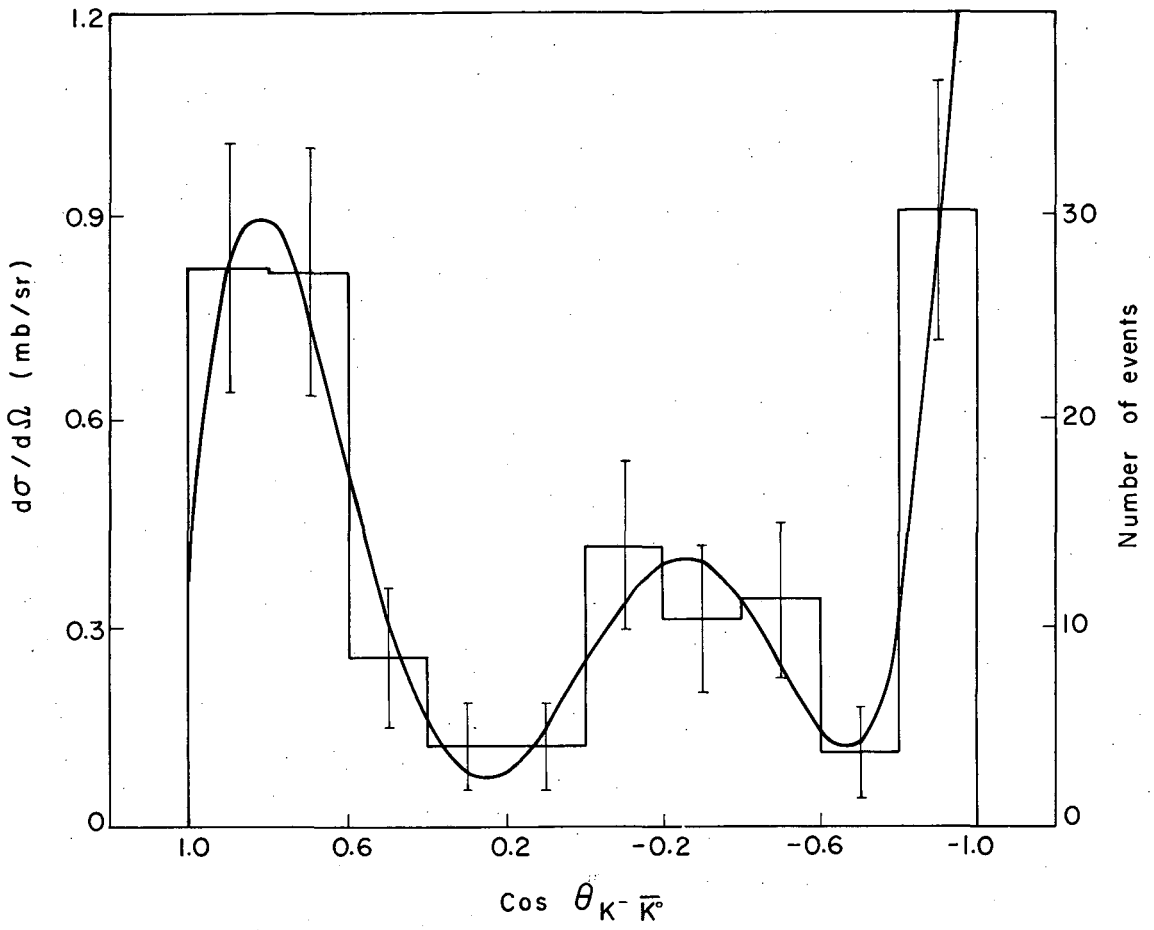

MUB-848

Fig. 5. Angular distribution of the $\overline{K^0}N$ events in the K^-p c.m. system. The curve represents a least-squares fit of the data to the first five Legendre polynomials.

B. Two-Prong Events

The analysis of our two-prong events is complicated because of the relatively large number of reactions that can produce this configuration. At our energy of 1.15 Bev/c, the following reactions can appear as two-prong events (Fig. 1) in a hydrogen bubble chamber:

$$K^- + p \rightarrow K^- + p \tag{7}$$

$$\rightarrow K^- + p + \pi^0 \tag{8}$$

$$\rightarrow K^- + \pi^+ + n \tag{9}$$

$$\rightarrow \pi^- + p + \overline{K^0} \tag{10}$$

$$\rightarrow \pi^- + \pi^+ + \begin{pmatrix} \Lambda \\ \Sigma^0 \end{pmatrix} \tag{11}$$

$$\rightarrow \pi^- + \pi^+ + \begin{pmatrix} \Lambda \\ \Sigma^0 \end{pmatrix} + \pi^0 \tag{12}$$

$$\rightarrow K + N \pm 2\pi \tag{13}$$

$$\pi^- + p \rightarrow \pi^- + p \tag{14}$$

$$\rightarrow \pi^- + p + \pi^0 \tag{15}$$

$$\rightarrow \pi^- + \pi^+ + n \tag{16}$$

$$\rightarrow N + 3\pi \tag{17}$$

Unfortunately, if an event fits a given K^- hypothesis at this momentum, it will usually fit also the corresponding π^- hypothesis, i.e. a $K^- + p \rightarrow K^- + p + \pi^0$ reaction will ordinarily give a satisfactory χ^2 to the $\pi^- + p \rightarrow \pi^- + p + \pi^0$ hypothesis. Moreover, the ambiguity cannot be resolved by inspecting the ionization of the outgoing particles, since the momentum of the negative track is usually in the region where both

π^- and K^- are minimum-ionizing. To reduce this difficulty, we decided to analyze the two-prong events only in the film sample in which the ratio of incident π^- to K^- particles was 0.08±0.11. This film sample, representing approximately 40% of our data, contained about 900 two-prong events.

We fitted each of these events to interpretations (7) through (11) and (14) through (16). The remaining reactions had two missing neutral tracks, and therefore could not be fitted. Since the fits to the elastic hypotheses (7) and (14) normally have four constraining equations, it is highly improbable that an inelastic event would fit an elastic interpretation. First, the two outgoing tracks would have to be coplanar with the incident track. This is very unlikely because the coplanarity at an event can be accurately checked (azimuth and dip errors for a typical track would be about 0.2 deg.) In addition to this, the event would have to satisfy the other three constraining equations. Accordingly the events were divided into two groups, elastic and inelastic, depending on whether they did or did not fit an elastic interpretation. Using this method to classify our reactions, we found approximately 600 elastic and 300 inelastic events.

For 29 of the 300 events that were classified as inelastic events, the momentum of one of the outgoing tracks was unmeasurable. These are primarily short tracks from events that occurred near one of the edges of the bubble chamber picture. Since these 29 events could not be fitted and were not biased with respect to the reaction that produced them, they were treated as unmeasurable inelastic events. In addition, 12 events were unmeasurable because of poor film quality or difficulties with the bubble chamber. All of the cross sections for the two-prong events have been corrected to take into account these two groups of unmeasurable events.

1. Elastic Events

The scanning efficiency for the elastic events depends upon the laboratory scattering angle and the orientation of the plane of the event. For scattering angles larger than 5 deg, our detection efficiency is very nearly 100%, regardless of the orientation of the scattering plane. Below 5 deg, the detection efficiency has a strong dependence on both the scattering angle and the plane of the event. Therefore we applied a cutoff angle and analyzed only the events with a scattering angle in the laboratory system greater than 10 deg. This corresponds to a recoil proton with a 2.5-cm range and to a $\cos\theta$ of 0.95 in the center-of-mass system.

The elimination of the events with $\cos\theta > 0.95$ left us with 511 events that fitted the K-p elastic hypothesis and 44 events that fitted only the π-p interpretation. Most of the 511 events that fitted the K-p elastic hypothesis also fitted the π^- interpretation. Therefore, to determine the number of K-p events, we had to estimate the number of π-p events that fitted the K-p interpretation.

To obtain an estimate of the total number of π^- elastic events, we examined the elastic scatters with $\cos\theta < -0.3$. Here θ is the angle, in the Kp (or πp) center-of-mass system, between the incident and final directions of the negative particle. In this cosine interval, the kinematics of the two reactions are sufficiently distinct so that none of these events fitted both π^- and K^- elastic interpretations. Nine of the 75 events with $\cos\theta < -0.3$ fitted the π-p hypothesis.

Using the fitted data on our elastic two-prong events, we found that the lower limit for the momentum spectrum of our π^- contamination was approximately 700 Mev/c. The upper limit was about 1150 Mev/c, since our beam would not accept a particle with a momentum larger than this. Fortunately, the angular distribution for π-p elastic scattering has been measured at 680,[9] 730,[9] 740,[10] 785,[10] 850,[9] 880,[9] 939,[11] 1000,[12] 1030,[9] 1045,[11] and 1150 Mev/c.[9] Using these angular distributions, we were able to estimate the value of R, the ratio of the number of events with $\cos\theta < -0.3$ to the number with $\cos\theta \leq 0.95$, for each of

the nine momenta at which the π-p two-prong events occurred. The ratio R varies quite slowly in this momentum interval ($0.15 \leq R \leq 0.30$). Using these ratios, we estimated that there were 38 ± 14 π-p elastic events with $\cos\theta \leq 0.95$. In a similar manner, we estimated 46 ± 16 for the total number of π-p elastic events.

Forty-four of our two-prong elastic events fitted only the π-p interpretation. However, some of these 44 events are probably Kp elastic reactions which failed to fit the Kp elastic hypothesis because they were produced by a low-momentum incident K meson. (As mentioned earlier, the measured momentum of the incident particle was averaged with 1150 ± 20 Mev/c for the K^- but not the π^- interpretation). From the study of our τ decays, we estimate that in about 2.5% (or 11 ± 5 events) of the K^-p elastic events the momentum of the incident K^- meson was low enough so that the event would not fit a K^-p elastic interpretation. Thus approximately 11 ± 5 of these 44 events are actually K^-p elastic scatters. Since we expect 38 ± 14 πp elastic scatters, only 5 ± 15 of the events that fitted the K^-p interpretation are π^-p elastic scatters. Thus our π^- contamination is quite small ($1 \pm 3\%$) and we shall neglect it in the discussions which follow. Table I summarizes the breakdown of the elastic events.

Figure 6 shows the angular distribution for the events that fitted the K-p elastic-scattering interpretation.

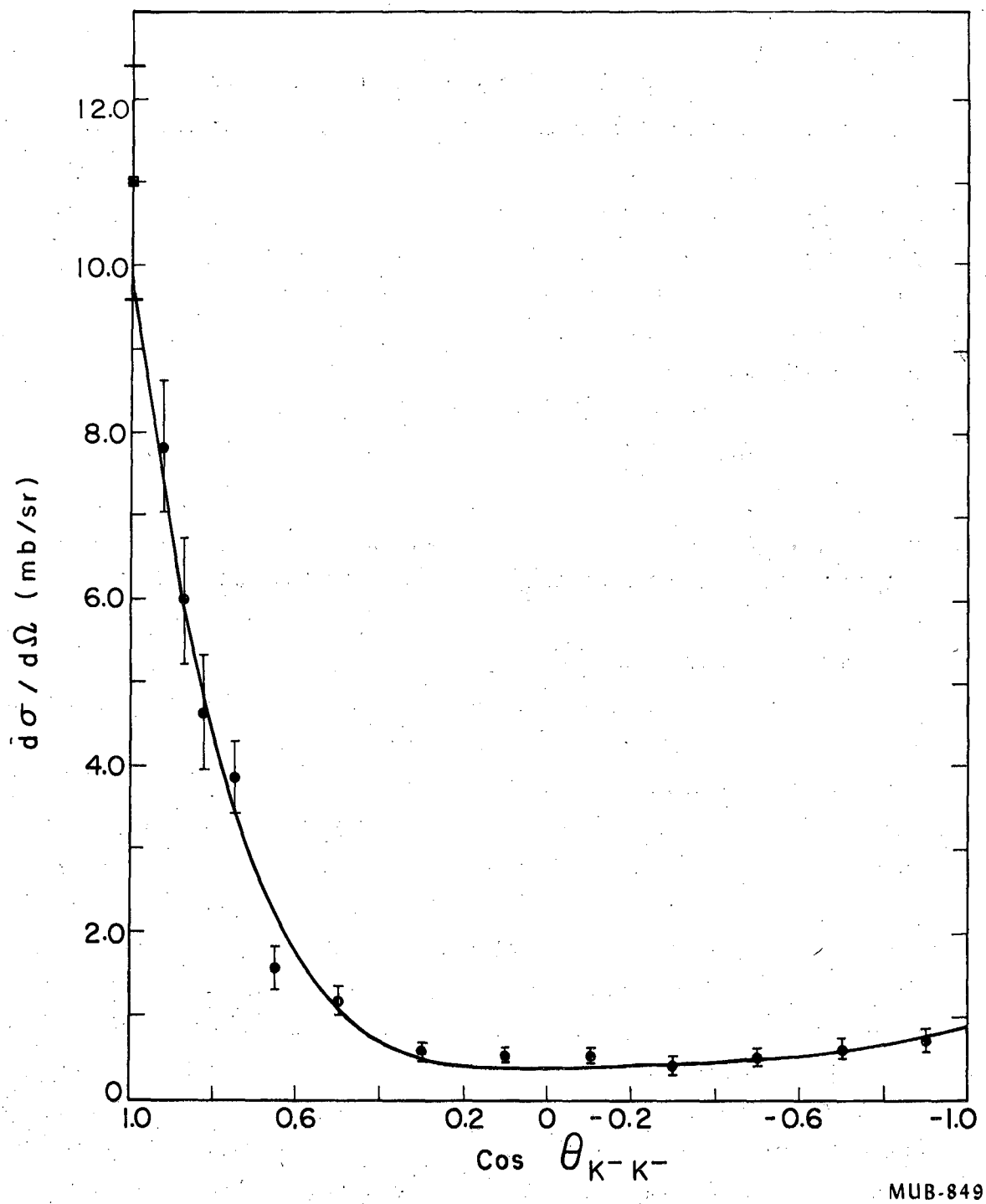

Fig. 6. Angular distribution for the $K^- + p \rightarrow K^- + p$ reaction in the c. m. system. A cutoff on the experimental data was imposed at $\cos\theta = 0.095$ (see text). The point at $\cos\theta = 1.0$ represents the square of the imaginary part of the forward-scattering amplitude; it was calculated using the optical theorem. The curve shown in the figure represents a least-squares fit of the data to the first five Legendre polynomials.

Table I. Summary of elastic events[a]

Total elastic scatters	555
Elastic scatters which fit the K^-p hypothesis	511
Elastic scatters which fit only the π^-p hypothesis	44
Low-energy K^-p elastic scatters which fit only the π^-p interpretation	11±5
π^-p elastic scatters	38±14
π^-p elastic scatters which fit the K^-p elastic-scattering interpretation	5±15

[a]Events with $\cos\theta > 0.95$ are not included in this table

2. Two-Prong Inelastic Events

Analysis of inelastic events is more difficult than that of elastic reactions, since more interpretations are possible, and the fits to these interpretations have only one independent constraining equation. An inelastic event, since it has only one constraint, will usually fit more than one interpretation. However, more information can be obtained about an event by looking at the ionization of the outgoing tracks. If the momentum of the positive track is below 800 Mev/c, we can ordinarily distinguish a π^+ meson from a proton by the ionization of the track. For a negative track with momentum up to approximately 400 Mev/c, we can usually distinguish a π^- meson from a K^- meson. Unfortunately, even after the inclusion of the information obtained from the ionization of the outgoing tracks, it is still impossible to decide upon an unambiguous interpretation for most of the inelastic events. The addition of the ionization data, however, does enable us to separate the inelastic two-prong events into two groups, group P and group π^+, depending on whether the positive track is a proton (group P) or a π^+ meson (group π^+). Thus the events due to reactions (8), (10), and (15) are in group P, while events due to reactions (9), (11), (12), and (16) are in group π^+.

To obtain the cross section for a given reaction, we must be able to estimate the number of events due to the other reactions in the same group. Accordingly, the following method is used to determine the cross sections for reactions (8) and (9):

1. We remove from group P the events that do not give a satisfactory fit to either hypothesis (8) or (15). From group π^+ we remove the events for which neither hypothesis (9) nor (16) yield a satisfactory fit.

2. In addition to producing inelastic two-prong events, reactions (10), (11), and (12) also produce V^0 two-prong events. These V^0 two-prong events are much less difficult to analyze than the inelastic two-prong events, and they have been studied in detail.[2,3] The data on these V^0 two-prong events are used to determine the number of events remaining in group P due to reaction (10) and the number remaining in group π^+ due to reactions (11) and (12).

3. The number of π-p elastic scatters is used to estimate the number of events in group P due to reaction (15) and the number in group π^+ due to reaction (16).

4. Finally, we estimate the number of events in the two groups due to reactions other than (8) through (12) and (14) through (16).

Table II shows the results of step 1 on the two groups.

Step 2 was performed by taking our V^0 two-prong events, disregarding the data on the V^0, and fitting the event to the two-prong interpretations [reactions (7) through (12) and (14) through (16)]. For each V^0 two-prong event that gives a satisfactory fit to one of the reactions (8), (9), (15), and (16), there will be $C(1-p)/p$ two-prong events in group π^+ or group P due to reactions (10) through (12). Here p is the probability of detecting a given event, which takes account both of the neutral decay mode of the V^0's as well as the escape probability. The factor C is the ratio of the number of K^- decays in the reduced film sample (π^- contamination is 0.08±0.11%) to the total number of K^- decays. That is, C corrects for the fact that these V^0 two-prong events were taken from the whole film sample, whereas the two-prong events were not. By this method we concluded that 47±7 of the events in group P were due to reaction (1) and 54±8 in group π^+ were due to reactions (11) and (12).

To estimate the number of $\pi^- + p \rightarrow \pi^- + p + \pi^0$ events in group P, and of $\pi^- + p \rightarrow \pi^- + \pi^+ + n$ in group π^+ (step 3), we used the number of π-p elastic scatters obtained in the analysis of the two-prong elastic events. The cross sections for $\pi^- + p \rightarrow \pi^- + p + \pi^0$ and $\pi^- + p \rightarrow \pi^- + \pi^+ + n$ have been measured at only two points in the momentum spectrum of our incident π^- mesons. Cross sections for π^- elastic scattering and for the above two reactions have been measured by Baggett[12] at 0.939 Bev/c and by Delano and Schmidt[13] at 1.0 Bev/c. The following ratios were calculated from their results:

Table II. Separation of two-prong inelastic events into groups P and π^+

	Group P	Group π^+
Events in each group	100	160
Events in group P(group π^+) which fitted either reaction (8) or (15)	94	154
Events in group P (group π^+) which fitted reaction (8) [(9)]	47	76
Events in group P (group π^+) which fitted reaction (15) [(16)] but not (8) [(9)]	47	78

$$V_1 = \frac{(\pi^- p \rightarrow \pi^- p \pi^0)}{(\pi^- p \rightarrow \pi^- p)} \quad \begin{array}{l} = 0.30 \pm 0.04 \text{ at } 0.939 \text{ Bev/c} \\ = 0.24 \pm 0.06 \text{ at } 1.0 \text{ Bev/c} \end{array}$$

$$V_2 = \frac{(\pi^- p \rightarrow \pi^- \pi^+ n)}{(\pi^- p \rightarrow \pi^- p)} \quad \begin{array}{l} = 0.76 \pm 0.06 \text{ at } 0.939 \text{ Bev/c} \\ = 0.47 \pm 0.11 \text{ at } 1.0 \text{ Bev/c.} \end{array}$$

Multiplying the value of V_1 and V_2, measured at 0.939 Bev/c, by the total number of elastic π-p events, we obtained 11±5 and 22±9 as the number of $\pi^- p \pi^0$ and $\pi^- \pi^+ n$ events, respectively. Using instead V_1 and V_2 measured at 1.0 Bev/c, we obtained 14±5 $\pi^- p \pi^0$ and 35±12 $\pi^- \pi^+ n$ events. Since the two estimates for the reactions are approximately within each others errors, we calculated their average and used these averages (12±5 and 27±8) for the number of events in groups P and π^+ due to the

reactions $\pi^- p \rightarrow \pi^- p \pi^0$ and $\pi^- + p \rightarrow \pi^- + \pi^+ + n$. Most of our π-p events are in the momentum interval from 850 to 1050 Mev/c, and therefore these averages should represent a reasonably accurate estimate for the number of π^- inelastic events.

Finally (step 4), we had to consider whether there was any significant contamination in groups P and π^+ due to special configurations of other reactions. Possible candidates are:

$\Sigma^{\pm}\pi^{\mp}(\pi^0)$ with a short $\Sigma^{\pm}$ (18)

$\Sigma^{\pm}\pi^{\mp}(\pi^0)$ with the $\Sigma^{\pm}$ decaying outside of the chamber (19)

$\Sigma^{\pm}\pi^{\mp}(\pi^0)$ with a small-angle Σ decay (20)

$\Lambda + n\pi^0$ $n \geq 1$ with a very short Λ (21)

$\Sigma^0 + n\pi^0$ $n \geq 1$ with a very short Λ (22)

$\overline{K^0} n (\pi^0)$ with a very short $\overline{K^0}$. (23)

These six categories represent special cases of reactions which we have analyzed previously (Ref 4 and Sections IIA and B). Using approximately the same method as in step 2, we were able to estimate the number of two-prong events in groups P and π^+ due to reactions (18) through (23). We estimated that 4±2 events in group P and 8±3 in group π^+ are examples of reaction (18), the contamination due to the other five reactions was found to be negligible.

The number of events due to reaction (13) is probably negligible, since in the entire film sample we have only one example of the reaction $K^- + p \rightarrow K^- + p + \pi^+ + \pi^-$ and no examples, among our V^0 two-prong events, of the reactions $K^- + p \rightarrow \overline{K^0} + p + \pi^- + \pi^+$ or $K^- + p \rightarrow K^0 + n + \pi^+ + \pi^-$.[3]

Thus the total number of events due to reactions other than (8) through (12) and (14) through (16) is 4±2 for group P and 8±3 for group π.

Table III contains a summary of the inelastic two-prong data. There are 94 events in group P. Of these events 47±7 are due to reaction (10) ($\overline{K^0}\pi^- p$); 17±8 are produced by reaction (15), and 4±2 are due to contaminating reactions. Thus of the 94 events in group P, 30±13 must be due to reaction (8). In a similar manner (see Table IV), we find that 65±15 of the 156 events in group π^+ are produced by reaction (9).

From Table II we can see that 78 of the 156 events in group π^+ are not consistent with a $K^-\pi^+n$ interpretation. (They are of course consistent with a $\pi^-\pi^+n$ interpretation.) Thus the 65±15 $K^-\pi^+n$ events must be contained in the remaining 76 events. Similarly, the 30±13 $K^-p\pi^0$ events are contained in 47 of the 94 events in group P. Therefore these 76 and 47 events form a reasonably pure sample for the $K^-\pi^+n$ and $K^-p\pi^0$ reactions, respectively.

Table III. Summary of inelastic two-prong data

	Group P	Group π^+
Events in each group	94±10	154±13
Events in Group P(group π^+) which fitted reaction (8)[(9)]	47±7	76±9
Events in Group P(group π^+) due to reaction (11) [(12) and (13)]	47±7	54±8
$\pi\pi N$ events in each group	13±5	27±8
Non-two-prong events in groups P and π^+	4±2	8±3
$K^-p\pi^0(K^-\pi^+n)$ events in group P(group π^+)	30±13	65±15

Table IV. Angular distribution of $\overline{K^0}N$ fitted to $f(\theta)=\sum_n A_n \cos^n\theta$

Order of fit	Value of A_n							Degrees of freedom	χ^2	Probability of exceeding χ^2 (%)
	A_0	A_1	A_2	A_3	A_4	A_5	A_6			
3	0.28 ±0.09	-0.11 ±0.32	1.08 ±0.40	1.01 ±0.62				6	28.8	1
4	0.46 ±0.12	-0.19 ±0.33	-1.15 ±0.93	1.00 ±0.64	3.29 ±1.27			5	22.1	1
5	0.41 ±0.09	-1.67 ±0.44	-0.26 ±0.75	9.50 ±2.06	1.92 ±1.02	-9.21 ±2.11		4	3.1	55
6	0.38 ±0.11	-1.61 ±0.43	0.54 ±1.73	9.01 ±2.12	0.38 ±5.85	-8.75 ±2.18	1.28 ±4.99	3	3.0	40

IV. RESULTS

A. $\overline{K^0}n$ and K^-p Reactions

Figure 6 shows the angular distribution for the events that fitted the reaction $K^- + p \rightarrow \overline{K^0} + n$. We fitted this distribution to a power series in cos θ. Reference 15 describes the method and the IBM 650 program used to perform the fits. Table IV lists, for each of the fits, the χ^2 value, the probability that a χ^2 as large as this would have occurred, and the values of the coefficients of the polynomials. A $\cos^5\theta$ term seems to be both necessary and sufficient to fit the angular distribution. The curve for the n = 6 fit, normalized to the total number of events, is plotted with the histogram for the angular distribution in Fig. 5. The cross section for the reaction $K^- + p \rightarrow \overline{K^0} + n$ at this energy is 5.3±0.5 mb.

Figure 6 contains the center of mass angular distribution for the $K^- + p \rightarrow K^- + p$ reaction. This distribution was also fitted to a power series in cos θ. The order of the fit, the values of the coefficients of the polynomials, the chi-square, the probability that a chi-square as large as this would have occured, and the value of $d\sigma/d\Omega$ at 0° are given in Table V for each of the fits. Here again n = 6 appears to be necessary to fit the angular distribution. The curve shown in Fig. 11 represents the n = 6 fit. The point at cos θ = 1.0 (11.0±1.0 mb/sr) represents the square of the imaginary part of the forward scattering amplitude. This was calculated from the total cross section at this energy (see end of Section IV) using the optical theorem.

To obtain the total number of K-p elastic scatters, we integrated the fitted curve (n = 6) from cos θ = - 1.0 to cos θ = 1.0 and made a small correction for the unmeasurable events. The K-p elastic scattering cross section is 18.3 ± 1.5 mb.

Table V. Elastic-scattering angular distribution for K^-p fitted to

$$f(\theta) = \sum_n A_n \cos^n\theta$$

Order of fit	Value of A_n								$d\sigma/d\Omega$ at 0 deg (mb/sr)	Degrees of freedom	χ^2	Probability of exceeding χ^2 (%)
	A_0	A_1	A_2	A_3	A_4	A_5	A_6	A_7				
3	0.10 ±0.02	-0.01 ±0.08	1.35 ±0.10	1.31 ±0.16					6.5±.3	9	33.2	1
4	0.15 ±0.04	-0.19 ±0.09	0.36 ±0.28	1.78 ±0.19	1.53 ±0.35				8.8±.7	8	13.5	9
5	0.16 ±0.03	-0.01 ±0.12	0.14 ±0.25	0.54 ±0.63	1.85 ±0.38	1.38 ±0.70			10.1±1.0	7	9.6	21
6	0.14 ±0.03	0.03 ±0.13	0.50 ±0.51	0.27 ±0.70	0.37 ±1.84	1.66 ±0.79	1.32 ±1.65		10.9±1.4	6	9.0	17
7	0.14 ±0.03	-0.09 ±0.19	0.58 ±0.51	1.84 ±1.84	-0.53 ±1.86	-2.91 ±0.50	1.74 ±1.68	3.51 ±3.81	12.2±1.9	5	8.1	15

B. KNπ Reactions

The analysis of our $\overline{K^0}p\pi^-$ events, with V^0 two-prong configuration, showed the existence of a $K\pi$ resonance, called K^{*3}. The mass of this resonance was found to be 885±3 Mev with a full width of 16 Mev after unfolding experimental errors. This corresponds to a lifetime of approximately 4×10^{-23} sec. The K^* resonance should display itself in our $K^-p\pi^0$, $K^-\pi^+n$, and $\overline{K^0}n\,\pi^0$ events. We would expect some of the $KN\pi$ reactions to have been produced by the following two-step processes:

$$K^- + p \rightarrow K^{*-} + p \qquad K^{*-} \rightarrow K^- + \pi^0$$
$$K^- + p \rightarrow \overline{K^{*0}} + N \qquad \overline{K^{*0}} \rightarrow K^- + \pi^+$$
$$\rightarrow \overline{K^0} + \pi^0 .$$

The characteristic feature of the K^* reaction is that the nucleon has a fixed kinetic energy of 20±4 Mev in the K-p center-of-mass system.

The distributions of the $K\pi$ masses for the $K^-p\pi^0$ and $K^-\pi^+N$ reactions are shown in Figs. 7 and 8. The solid curves in those figures represent the mass distribution predicted by phase space and normalized to the total number of events. The peak in the mass distributions in the two figures at 885 Mev indicates the presence of K^* events in both of these reactions. The dashed phase-space curves in the two figures are normalized in the interval $M_{K\pi} < 835$ Mev, and thus represent the three-body background.

To determine the number of K^* events, we took the number of events in the mass interval 885±30 Mev (the error on the $K\pi$ mass ranges from about 10 to 30 Mev) and, using the dashed curves, subtracted the number of events due to the background. The result is 14±4 $K^{*-} \rightarrow K^- + \pi^0$ and 19±5 $K^{*0} \rightarrow K^- + \pi^+$ events. These numbers correspond to cross sections of 0.48±0.14 mb and 0.64±0.17 mb, respectively (including corrections of unmeasurable events).

The isotopic spin of the K^* can be determined from the value of the branching ratio R, where

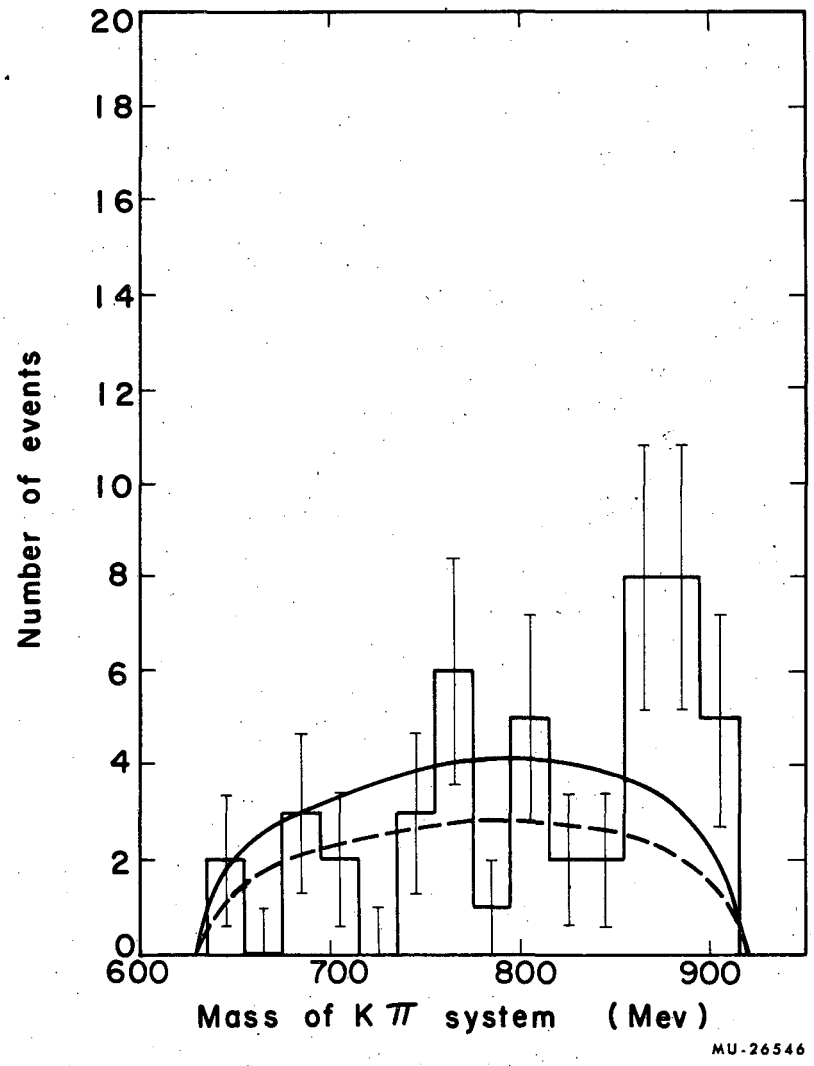

Fig. 7. Mass spectrum of $(K^- \pi^0)$ system.[1] The solid curve represents the distribution, normalized to the total number of events, that would be expected if the reaction followed phase space. The dotted curve is normalized to the background (see text).

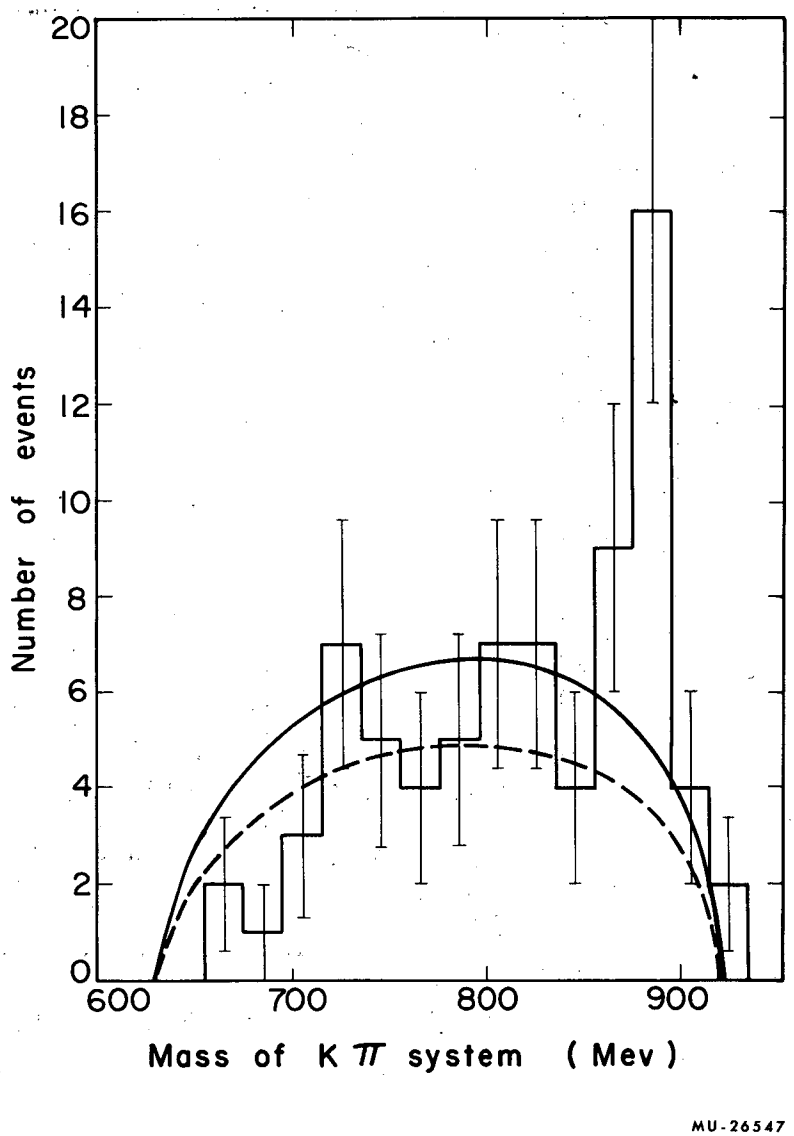

Fig. 8 Mass spectrum of $(K^- \pi^+)$ system. The solid curve represents the distribution, normalized to the total number of events, that would be expected if the reaction followed phase space. The dotted curve is normalized to the background (see text).

$$R = \frac{K^{*-} \rightarrow K^- + \pi^0}{K^{*-} \rightarrow \overline{K^0} + \pi^-} .$$

If the isotopic spin of the K^* is 1/2, R equals 1/2; if the isotopic spin is 3/2, R equals 2. In the analysis of our V^0 two-prong events, we found that the cross section for K^{*-} events, in which the K^{*-} decays into $\overline{K^0} + \pi^-$, was 0.9±0.2 mb.[3] Using the cross section for K^{*-} events, in which $K^{*-} \rightarrow K^- + \pi^0$, we obtained a value for R of 0.5±0.2. We therefore concluded that the isotopic spin of the K^* is 1/2. This agrees with an earlier preliminary analysis, which was also based on these two-prong inelastic events.[3]

Since the $\overline{K^0} n \pi^0$ events cannot be fitted, it was not possible to obtain a Dalitz plot for this reaction. Thus we could not obtain information about the $K^{*0} n$ reaction from our $\overline{K^0} n \pi^0$ events.

The first pion-nucleon resonance (mass = 1238 and Q = 90 Mev) could also effect these $KN\pi$ reactions. Its presence would be indicated by a concentration of events along the horizontal lines on the Dalitz plots, where T_K=90 Mev (see Figs. 9 and 10). No peaking in this region is observed, but this is a rather wide resonance and would therefore be difficult to detect because of the background events and our limited statistics.

In reference 3, which contains the discussion of our $K^- + p \rightarrow \overline{K^0} + p + \pi^-$ events, evidence was presented for the hypothesis that the K^* has spin less than two. This evidence was based on the assumption that the K^*N system is in a state of zero orbital angular momentum. There are two justifications for this assumption. One is that we are only 35 Mev above the K^*N threshold; the other is that the K^*N angular distribution is consistent with isotropy. If the assumption of S-wave production for the K^*N system is valid, the following relations involving $\overline{\cos^2\theta}$ can be derived (see reference 3 for the method):

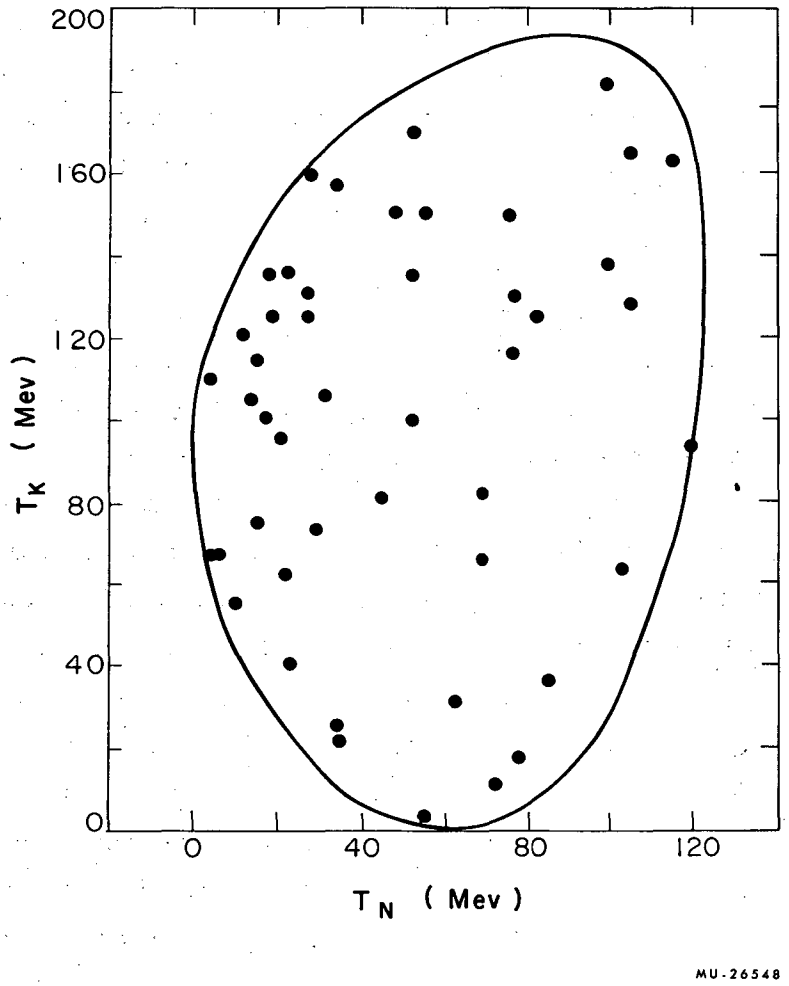

Fig. 9. Dalitz plot for the reaction $K^- p \pi^0$.

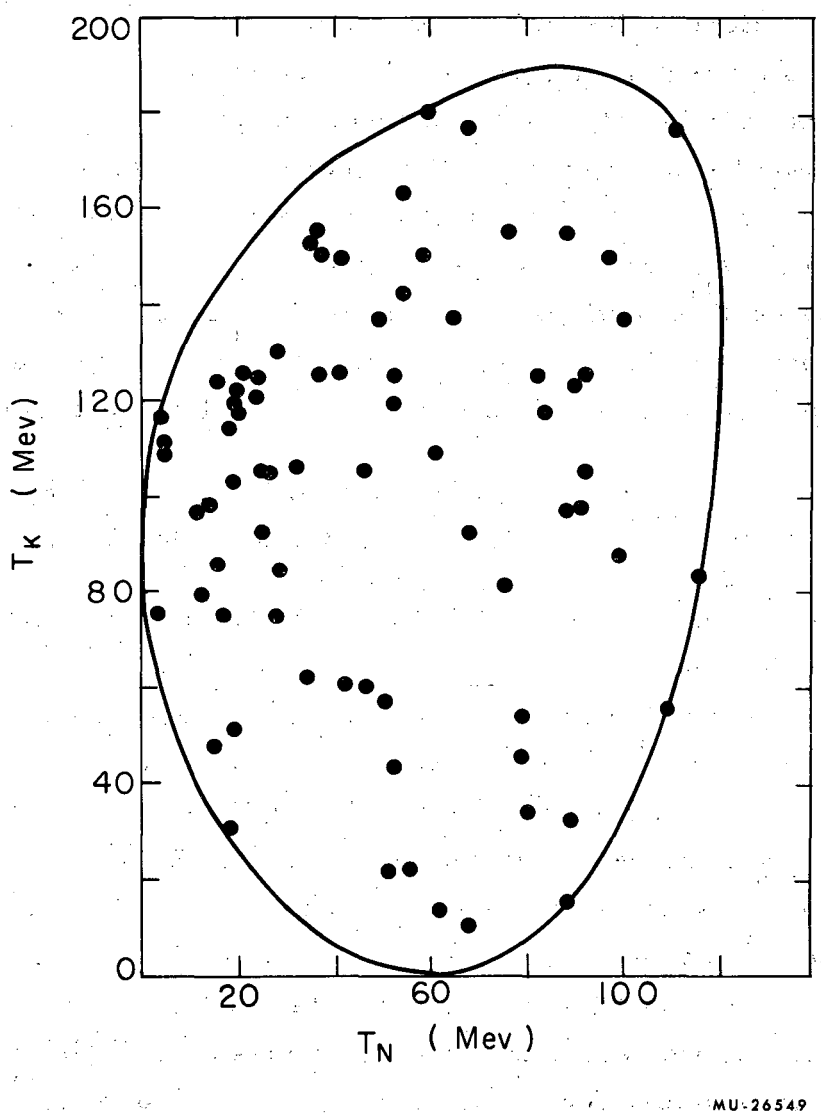

Fig. 10. Dalitz plot for the reaction $K^- \pi^+ n$.

$$\overline{\cos^2\theta} = 0.33 \quad \text{for } K^* \text{ spin} = 0$$
$$0.20 < \overline{\cos^2\theta} < 0.60 \quad \text{for } K^* \text{ spin} = 1$$
$$\overline{\cos^2\theta} > 0.429 \quad \text{for } K^* \text{ spin} > 1 .$$

Here θ represents the angle in the K^* rest system that the π meson makes with the incident K^- direction. Except for the $S = 0$ case, the exact value of $\overline{\cos^2\theta}$ depends on the mixture of $J = S+1/2$ and $J = S-1/2$ states in the K^*N system (S is the spin of K^*).

In our $K^-p\pi^0$ and $K^-\pi^+N$ events, we had 21 and 29 events, respectively, in the K^* peak, of which 14±4 of the 21 and 19±5 of the 29 were K^* reactions. The angular distributions of the 21 and 29 events are both consistent with isotropy; this agrees with the hypothesis of an S-state K^*N system. We obtained the following results for $\overline{\cos^2\theta}$:

$$\overline{\cos^2\theta} = 0.39\pm0.07 \quad \text{for } 21\ K^-p\pi^0 \text{ events}$$
$$= 0.43\pm0.05 \quad \text{for } 29\ K^-\pi^+N \text{ events.}$$

In reference 3 we had $\overline{\cos^2\theta} = 0.275\pm0.05$ for 26 $\overline{K^0}p\pi^-$ events (22±2 were K^* events).

The value of $\overline{\cos^2\theta}$ for the $K^-p\pi^0$ events can be averaged with that for the $\overline{K^0}p\pi^-$ events of reference 3, since they are both examples of $K^{*-} + p$ reactions. The result is 0.31±0.04. Thus taking either the $\overline{K^0}p\pi^-$ data alone or averaging it with the $K^-p\pi^0$ data, we find a value for $\overline{\cos^2\theta}$ which is three standard deviations from the value expected for a K^* with a spin greater than one. Since the mixture of $J = S+1/2$ and $J = S - 1/2$ states could be different for the K^* reactions, we cannot average the values of $\overline{\cos^2(\theta)}$ obtained from the two reactions unless $S = 0$. Averaging the K^{*-} and K^{*0} data yields a result, 0.36±0.3, which is consistent with $S = 0$.

From the value of $\overline{\cos^2\theta}$ for the 26 $\overline{K^0}p\pi^-$ events, we concluded, in reference 3, that the K^* probably does not have a spin greater than one. Unfortunately, from the results for the 21 $K^-p\pi^0$ and the 29 $K^-\pi^+n$ events, we cannot obtain any additional information about the K^* spin. However, the addition of the $K^-p\pi^0$ and $K^-\pi^+n$ data to the $\overline{K^0}p\pi^-$ data does not alter the conclusion that the K^* probably has a spin less than two.

Using the branching ratios for the $K^*(I=1)$, we calculated the cross sections for $K^- + p \rightarrow K^{*-} + p$ and $K^- + p \rightarrow K^{*0} + n$. These cross sections, including corrections for unmeasurable events, are shown in Table VI. The cross sections for $K^- p \pi^0$, $K^- \pi^+ n$, and $\overline{K^0} n \pi^0$, including K^* events (and corrections for unmeasurable events) are also given in Table VI.

The total $K^- p$ cross section at 1.15 Bev/c, obtained by combining the results of references 2, 3, and 4 with the results of this paper, is 45±2 mb. Table VI contains a summary of the cross sections discussed in this paper.

Table VI. Summary of non hyperonic $K^- p$ interactions at 1.15 Bev/c

$K^- p$ reaction	Cross section
$K^- + p$	18.3±1.5
$\overline{K^0} + N$	5.3±0.5
$K^{*-} + p$	1.35±0.3
$K^{*0} + N$	0.91±0.15
$K^0 + p + \pi^0$ [a]	1.0±0.4
$K^- + \pi^+ + n$ [a]	2.1±0.5
$\overline{K^0} + n + \pi^0$ [a]	1.3±0.3
$\overline{K^0} + p + \pi^-$ [a, b]	2.0±0.3

[a] The $KN\pi$ cross sections include the K^* events.

[b] Data for $\overline{K^0} + p + \pi^-$ reactions are from reference 3.

ACKNOWLEDGMENTS

I would like to thank Profs. Luis W. Alvarez, Myron L. Good, Arthur H. Rosenfeld, and Harold K. Ticho, as well as Drs. Margaret H. Alston, Philippe Eberhard, and Stanley Wojcicki for generous contributions of their time and effort and for their valuable advice given during the course of this experiment.

I am indebted to Profs. Arthur H. Rosenfeld, James Snyder, and Horace Taft; Drs. Frank Solmitz, Ronald Ross, and William Humphrey; and Mr. Jon Peter Berge for the development of the PANG and KICK digital-computer programs.

The cooperation of the Bevatron crew under the direction of Dr. Edward Lofgren, and of the bubble-chamber crew under the direction of Messrs. Donald Gow, Robert Watt, and Glenn Eckman is gratefully acknowledged.

Finally, I would like to thank the scanners who participated in this experiment, especially Messrs. Joseph Waldman and Jon Folkman.

This work was done under the auspices of the U. S. Atomic Energy Commission.

REFERENCES

1. L. W. Alvarez, P. Eberhard, M. L. Good, W. Graziano, H. K. Ticho, and S. G. Wojcicki, Phys. Rev. Letters 2, 215 (1959).
2. M. Alston, L. W. Alvarez, P. Eberhard, M. L. Good, W. Graziano, H. K. Ticho, and S. Wojcicki, Phys. Rev. Letters 5, 520 (1960).
3. M. Alston, L. W. Alvarez, P. Eberhard, M. L. Good, W. Graziano, H. K. Ticho, and S. Wojcicki, Phys. Rev. Letters 6, 300 (1961).
4. M. Alston, L. W. Alvarez, P. Eberhard, M. L. Good, W. Graziano, H. K. Ticho, and S. Wojcicki, Phys. Rev. Letters 6, 698 (1961).
5. P. Eberhard, M. L. Good, and H. K. Ticho, Rev. Sci. Instr. 31, 1054 (1960).
6. Stanley G. Wojcicki, Pion Hyperon Resonances, UCRL-9835 (thesis), August 24, 1961.
7. Jack V. Franck, Franckenstein - Semi-Automatic Measuring Projector, UCRL-8378, November 20, 1961.
8. William E. Humphrey, A Description of the PANG Program, Alvarez Group Memo 111, September 18, 1959, and Memo 115, October 25, 1959 (unpublished); Arthur H. Rosenfeld, "Digital-Computer Analysis of Data from Hydrogen Bubble Chambers at Berkeley," in Proceedings of the International Conference on High-Energy Accelerators and Instrumentation, CERN, 1959 (CERN, Geneva, 1959).
9. A. H. Rosenfeld and J. N. Snyder, Digital-Computer Analysis of Data from Bubble Chambers, IV. The Kinematic Analysis of Complete Events, UCRL-9098, February 16, 1960 (Rev. Sci. Instr. 33, 181 (1962); J. P. Berge, F. T. Solmitz, and H. Taft, Rev. Sci. Inst. 32, 538 (1961).
10. C. Wood, T. Devlin, J. Helland, M. Longo, B. Moyer, and V. Perez-Mendez, Phys. Rev. Letters 6, 481 (1961).
11. John I. Shonle, Differential Elastic Pion-Proton Scattering at 600, 650, and 750 Mev (Thesis), August 12, 1960.

12. Lee Baggett, Jr., π^--p Elastic Scattering and Single-Pion Production at 0.939 Bev/c, UCRL-8302 (thesis), May 28, 1958.

13. I. Derado and N. Schmitz, Phys. Rev. 118, 309 (1960).

14. S. Bergia, L. Bertocchi, V. Borelli, G. Broutti, L. Chersovani, L. Lavatelli, A. Minguzzi-Ranzi, R. Yosi, P. Waloschek, and V. Zoboli, Nuovo cimento 15, 551 (1960).

15. Lester K. Goodwin, A General Least-Squares Program for the IBM 650 Computer, UCRL-9263, June 14, 1960.